Earth Surface Processes and Landforms
Earth Surf. Process. Landforms, **23**, 791–808 (1998)

BED MATERIAL TRANSPORT ESTIMATED FROM THE VIRTUAL VELOCITY OF SEDIMENT

JUDITH K. HASCHENBURGER*† AND MICHAEL CHURCH
Department of Geography, The University of British Columbia, Vancouver, British Columbia, Canada V6T IZ2

Received 12 February 1997; Revised 19 December 1997; Accepted 7 January 1998

ABSTRACT

This study evaluates the possibility of determining bed material transport using the virtual rate of travel of individual particles, dimensions of the active layer of the streambed, and porosity and density of streambed material. Magnetically tagged stones and scour indicators were employed in Carnation Creek, British Columbia, to quantify transport rates. Observations cover flows up to $36\,m^3\,s^{-1}$ ($\tau^* = 0{\cdot}081$). Tranport rates, ranging from $0{\cdot}090$ to $9{\cdot}7\,kg\,s^{-1}$ ($0{\cdot}12$–$13{\cdot}2\,m^3\,h^{-1}$), display a relatively sensitive trend with maximum stream power, as expected. Error analysis indicates that uncertainty in virtual velocity covers the majority of sample variance. An evaluation of the two measurement techniques used to delineate active layer dimensions, magnetically tagged stones and scour indicators, indicates that they yield comparable depths, widths and transport rates over the range of flows observed. Issues for further study are discussed. © 1998 John Wiley & Sons, Ltd.

KEY WORDS: active layer; bed material; fluvial sediment transport; gravel-bed channel; scour; tracers

INTRODUCTION

Transport rates of bed material in gravel-bed channels are typically quantified during floods by using portable sediment samplers (Hubbell, 1964; Helley and Smith, 1971; Engel and Lau, 1981) or pit-type traps (Milhous and Klingeman, 1973; Emmett, 1980; Reid *et al*., 1980) to sample the sediment flux at fixed cross-sections. Spatial and temporal variability in bed material transport (Ergenzinger, 1988; Hoey, 1992), however, complicates the acquisition of representative data (Hubbell and Stevens, 1986). When a sufficiently wide range of conditions is sampled, a scale correlation can be developed between transport rates and flow conditions. Discharge (Schoklitsch, 1934; see Shulits, 1935), shear stress (du Boys, 1879) and stream power (Bagnold, 1966, 1986) are commonly selected to represent flow conditions (see reviews in Graf, 1971; Gomez, 1991).

An alternative approach to determine transport rates (Einstein, 1937; Hubbell and Sayre, 1964) uses information about the virtual velocity of particle movement, dimensions of the active layer of the streambed, and the porosity and density of the bed material. Virtual velocity is defined as the total distance travelled (possibly incorporating multiple steps) by individual grains divided by the measurement interval, typically the total time of competent flow during a flood event. The active layer constitutes the portion of the streambed that is mobilized during floods competent to transport sediment. Its dimensions vary spatially and temporally (Hollingshead, 1971; Hassan, 1990; Haschenburger, 1996; Wilcock *et al*., 1996). Field observations of these quantities are, in general, difficult to obtain. Consequently, estimation of transport rates using this steady-state sediment continuity approach has seen limited field application. In studies by Mosley (1978), Kondolf and Mathews (1986) and Carling (1987), transport estimates include one or more approximations of input variables which were not measured directly in the field. Moreover, most investigations (see also Hassan *et al*., 1992; Laronne *et al*., 1992) have been restricted to one flood event.

The objective of this paper is to evaluate the possibility of developing a transport–flow relation using the virtual velocity approach to estimate bed material transport. The investigation entails quantifying transport rate

* Correspondence to: Judith K. Haschenburger, Department of Geography, The University of British Columbia, Vancouver, British Columbia, Canada V6T 1Z2.
† Present address: Department of Geography, The University of Auckland, Private Bag 92019, Auckland, New Zealand
Contract/grant sponsors: Natural Sciences and Engineering Research Council of Canada; Geological Society of America

CCC 0197-9337/98/090791–18

over a range of flows in a single gravel-bed river using magnetically tagged bed material and scour indicators. The observations permit comparison of two measurement techniques to define the active layer of the streambed. Since the technique remains in a development stage, an extended discussion is given of errors, approximations, and issues for further study.

ESTIMATION OF BED MATERIAL TRANSPORT

A fundamental equation for the mass rate of transport of bed material, G_b, is given by:

$$G_b = v_b\, d_s\, w_s\, (1-p)\, \rho_s \tag{1}$$

where v_b is the mean virtual travel rate of bed material ($m\,h^{-1}$), d_s the active depth of the streambed (m), w_s the active width of the streambed (m), p the fractional porosity of channel sediment, and ρ_s the mineral density of sediment (kg m^{-3}), which is commonly taken as 2650 kg m^{-3}. Transport estimates derived from Equation 1 characterize bed material that has moved relatively short distances by traction, saltation, or in suspension, and originated from the channel bed and the lower portion of channel banks (Martin and Church, 1995).

Virtual velocity incorporates periods of both rest and motion experienced by individual particles and therefore is less than the actual velocity during particle movements. Virtual velocity directly covers the random aspect of particle movement in the estimation of transport rates. Previous work suggests that both the active depth and width of the streambed vary with flow magnitude (Hollingshead, 1971; Slaymaker, 1972; Madej, 1984; Haschenburger, 1996) and therefore these variables should not, in general, be treated as constants in the determination of bed material transport over a range of flow conditions (but see later discussion on the variation of active width).

In this study stream power, Ω, is used to represent flow strength and is given by:

$$\Omega = \rho\, g\, Q_p\, S \tag{2}$$

where ρ is the fluid density (kg m^{-3}), g the acceleration due to gravity ($m\,s^{-2}$), Q_p the flood peak discharge ($m^3\,s^{-1}$), and S the channel slope ($m\,m^{-1}$). Stream power, expressed as the rate of energy dissipation per unit length of channel, is the most appropriate index of work accomplished to move sediment because transport rates are based on a group of particles travelling through a length of channel. Selection of peak discharge for stream power calculations emphasizes the disproportionate importance of the highest flows, which arises from the non-linear increase in transport with flow magnitude (in fact, highly non-linear for the near-threshold conditions characteristically encountered in most gravel-bed channels).

STUDY SITE

Carnation Creek, a small gravel-bed stream that drains about 11 km^2, is located on the west coast of Vancouver Island, British Columbia (Figure 1). Mean annual precipitation is about 3200 mm, delivered primarily between October and March by frequent cyclonic storms. Although snow is occasionally received at higher elevations, it constitutes only 5 per cent of the total precipitation. Hydrologic response to storm events is rapid, resulting in flood hydrographs with short time-to-peak. Continuous flow data are available from a stream gauge near the basin outlet (Water Survey of Canada gauge 08HB048). A secondary stage recorder was installed for this study (Figure 1) about 2 km upstream.

In the study reach, channel planform consists of relatively straight reaches punctuated by sharp bends. Resistant bank material or bedrock frequently force the bend configuration. Organic debris and bedrock outcrops (Lisle, 1986) appear to exert some influence on the location of pool–riffle–bar units, although avalanche faces on gravel bars suggest some downstream mobility. Bankfull width and depth average 15 and 0·8 m, respectively. Surface and subsurface bed materials have median diameters of 47 and 29 mm; D_{84} is 97 and 89 mm, whilst D_{16} is 19 and 3·6 mm.

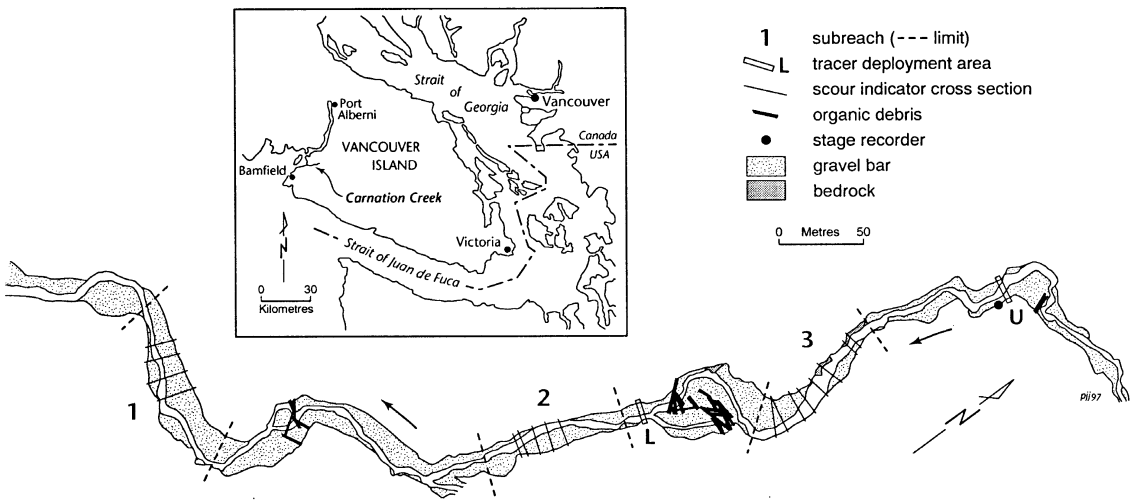

Figure 1. The study reach in Carnation Creek, showing subreaches, scour indicator cross-sections, and tracer deployment areas

Table I. Description of subreaches in Carnation Creek

Subreach	Distance from lower limit of study reach (m)	Subreach length (m)	Mean active bed width (m)	Mean bankfull width (m)	Bed gradient (%)	Distance from tracer deployment area (m)*		Number of scour indicators	Indicator type‡
						Upper	Lower†		
1	103	100	17·6	18·3	1·20	675	385	26	SC
2	392	90	10·5	12·2	1·17	390	100	21	SC
3	599	100	9·7	11·7	0·56	190	N/A	36	SM

* Distance determined from downstream limit of subreaches
† Lower deployment area used only prior to second flood season
‡ SC, scour chain; SM, scour ball monitor

PROGRAMME OF OBSERVATIONS

Field measurements were concentrated in three relatively straight subreaches within the 900 m long study reach (Figure 1). In these subreaches (Table I), active cross-sectional dimensions can be delineated using both magnetically tagged stones and scour indicators. Estimation of virtual velocity relies upon tracing marked stones. With estimates of sediment porosity and density, computations using Equation 1 can then be completed.

Tracer particles

Determination of virtual velocity requires measurements of travel distance of individual particles, which are derived from knowing the positions of magnetically tagged stones before and after flood events, and either direct documentation or estimation of the total time particles might be in motion during floods. The tracers used to determine travel distance must be representative of the sediment body of interest moving within the active layer (Hubbell and Sayre, 1964). Since the size of mobile sediment in gravel-bed channels corresponds with the distribution of subsurface material rather than of surface material (e.g. Parker and Klingeman, 1982), the tracer size distribution should mimic the subsurface size distribution. Approximately 1000 tracers were deployed in the study reach (Table I) prior to each of two flood seasons. Tracer size fractions ranged from 16 to 180 mm. Strictly, then, the observations reflect the movement of the upper 63 per cent of the subsurface bed material size distribution. We suppose that this material, or some fraction of it, controls bed stability.

We have no direct measurements of the commencement and cessation of particle motion. Indeed, such conditions are difficult to define in stream channels (Wilcock, 1993). A selected baseline discharge of $4\,m^3\,s^{-1}$ defined the period of sediment mobility for the purpose of computing virtual velocities. During the field programme scour indicators recorded a mean scour depth of less than 1 cm over the full width of the channel bed in response to a flood peak of about $4\,m^3\,s^{-1}$, while visual observations at $2{\cdot}7\,m^3\,s^{-1}$ documented an immobile bed in subreach 2. Further, prior to this study, a sediment transport rate of $0{\cdot}015\,kg\,s^{-1}$ was determined for a channel section located near the WSC streamflow gauging station at a corresponding discharge (Tassone, 1987). When this rate is converted into a unit width flux it is comparable to the dimensionless reference transport rate of 0·002 commonly used in sediment flux calculations (Wilcock, 1993). Asymmetry between the initiation and cessation of sediment transport (Reid and Frostick, 1984) was not investigated in Carnation Creek. If such conditions occur, they would have to create relatively large differences in the defined time period in order to modify velocities beyond the standard deviations associated with the virtual velocity estimates (discussed below).

Burial depths of individual tracers constitute observations for estimating active depth within each subreach. Tracers mobilized from known channel positions and burial depths document, in general, the minimum depth of streambed scour achieved during a given flood. Scour may continue beyond the depth necessary to entrain a given tracer, but this bed activity cannot be recorded unless another tracer resides at a deeper depth in the same channel position and is also scoured. At a limited number of channel locations, the recorded scour depth might be expected to correspond to the maximum depth of the active layer (Hassan and Church, 1994). Burial depths associated with tracers deposited during a flood record a net fill depth since the time of tracer emplacement. Observations from all mobile tracers, even those on the surface, help to define the active layer. In contrast, tracers initially on the surface that remain in place and on the surface after a flood document locations on the streambed that did not experience scour or fill activity, even within a generally active transport zone.

A consistent reference level for measuring burial depth to the bottom of tracers was established by using a T-shaped measuring device, the crossbar of which rested on the bed surface. Measurements are therefore referred to a locally averaged top elevation of bed surface particles. Measurement error associated with burial depths is estimated at ±2 cm, due in part to the difficulty of specifying excavated tracer position precisely in the wetted channel. Scour and fill depths used in defining active depth are burial depths adjusted to the midpoint of the particle vertical axis, which typically is the c-axis based on field observations. Tracers buried deeper than the detection limit of the magnet detector used for recovery, about 1 m, could not be located and introduce some unquantified bias into estimates of active layer dimensions and virtual velocity. Overall, depths derived from tracers are most likely lower bound estimates of the active layer depth. The positions at which depths are determined varies, of course, from event to event, depending on where tracers happen to come to rest. Further, when more than one flood occurred between resurveys, derived depths are based on tracers found in a collection of channel positions that may have been determined in part by each event.

Active width corresponds to the lateral dimension of the zone of bed material transport in a channel. This zone was determined for a given flood by plotting initial and final locations of mobile tracers on planimetric maps of the channel, delineating lateral boundaries of activity, and extracting 10 cross-sectional width estimates to characterise active width. Stationary tracers on the surface helped guide zone delineation in some areas. In other areas, however, bed activity may continue some distance beyond the locations of tracers that signify movement, especially if the bounding tracers are buried. Therefore, a buffer of probable bed activity was incorporated into active width estimates and was set at 1 m per boundary to maintain consistency with widths derived from scour indicators (discussed below). Confidence in width delineation increases with the number of tracers within a given channel reach. Widths can be derived separately for scour and fill activity.

Scour indicators

Delineation of active layer dimensions using scour indicators involved deployments along a number of channel cross-sections located within each subreach (Table I). In each cross-section, scour indicators were spaced at 2 m intervals, in general, and spanned the complete channel width between banks. Indicators were positioned in pool, riffle and bar areas of the bed. Installation of individual scour indicators required from 10 min to nearly 2 h, depending on bed conditions, with the aid of a rock drill coupled with a double pipe driver that

accelerated insertion and facilitated deployment in the wetted channel. Using the driver minimized bed disturbance compared to excavating a hole. However, as the driver penetrated the streambed, it moved a sediment column at least 6 cm in diameter to the depth of insertion, which was usually 1 m.

The two types of scour indicators employed in this study, metal-link scour chains (Leopold *et al*., 1966; Laronne *et al*., 1994) and scour ball monitors (Tripp and Poulin, 1986), produce comparable data, although the latter type records depth in 4 cm increments. The T-shaped measuring device provided a consistent reference level for scour chain measurements and facilitated data collection in the deep portion of the flow channel. Measurements of scour ball monitors involved counting the number of 4 cm diameter balls liberated during the flood event and the number of balls replaced into the bed when the top ball was flush with the surface. Error in measurements of scour and fill depths based on scour chains is ±1 cm while the estimated measurement error associated with scour ball monitors is ±2 cm.

Scour indicators register the maximum scour depth and net fill depth at the location of the indicators and record only one apparent cycle of scour and fill between resettings. The insertion depth of indicators into the streambed dictates the maximum observation of scour depth that can be recorded. As long as scour indicators remain in place, there is no inherent limitation to the net fill depth that can be measured. In contrast to tracers, scour indicators provide depth observations in fixed locations of the channel and delineate the maximum extent of the active layer at these locations.

Definition of the active width is based on those indicators that record bed activity within instrumented cross-sections. Given the lateral spacing between scour indicators, some termination of activity must be determined or estimated. Hence, in each cross-section, bed activity was assumed to continue 1 m toward the adjacent inactive indicator (i.e. midway) or bank edge for both lateral boundaries. During some flood periods, more than one distinct zone of scour activity was recorded within a given cross-section. The amount of uncertainty introduced into estimated active widths depends in part, then, on the spacing of scour indicators.

TRENDS IN VARIABLES

Over two flood seasons, recoveries of tracers and scour indicators permit computation of variables and transport rates for three individual flooding periods in subreaches 1 and 2 and six flooding periods in subreach 3 (Table II). The reduced number of computations for subreaches 1 and 2 reflects an insufficient number of tracers to determine virtual velocity and active layer dimensions in these two subreaches. In each recovery, only a small proportion of the total population of tagged stones turned up in each measurement reach (typically 5 to 15 per cent; see Table II). The data are used to calculate mean results and, for this purpose, the numbers are probably adequate (see discussion by R. I. Ferguson in Hassan and Church, 1992). The sequence and spatial extent of tracer recoveries during the field programme dictated that velocities be derived from mean travel distances that represent, in general, sediment moving into and within a subreach or moving within and out of a subreach.

Of the six flooding periods, four can readily be considered to be dominated by one flood event (Table II) because either the flooding period contained only one discrete flood hydrograph or the additional events within the flooding period were relatively small compared to the maximum peak event and hence are expected to have had little effect on total travel distances. For the remaining two flooding periods, with multiple events, the peak of the largest flood was not significantly greater than the peak of a second flood, which suggests that travel distances should be adjusted prior to calculating virtual velocities for these two periods. Thus, distances were reduced by the ratio of the maximum peak discharge to the sum of the two largest peak discharges within each flooding period. Any additional floods were of insufficient magnitude to transport significant amounts of bed material. The depth and width of the active layer should register the maximum fluctuation produced by the most effective flood peak, which is assumed to be the maximum peak, given a relatively stable channel. Overall, Carnation Creek maintained a relatively constant mean bed elevation during the monitoring programme (Haschenburger, 1996).

Virtual velocity

Virtual velocity tends to increase with stream power (Figure 2) but the relation is not at all strict. Apart from the observations of newly placed, unconstrained tracers (adjustment of which is discussed in the figure caption),

Table II. Variables for computation of bed material transport rates, Carnation Creek

Flooding period[a]	A	B	C	D	E	F
Dominant peak discharge ($m^3 s^{-1}$)[b]	24·5	30·4	*22·6*	17·7	36·3	*17·9*
Duration of competent flow (h)	32·5	25·8	27·2	14·8	21·6	19·8
Dimensionless shear stress[c]	0·065	0·073	0·062	0·054	0·081	0·054
Subreach 1[d]						
Stream power ($W m^{-1}$)				2360	5090	2250
Mean travel distance (m)[e]				82·6[f]	125·9[f]	48·7[f]
Number of mobile tracers[g]				8	29	7
Virtual velocity ($m h^{-1}$)				2·9[h]	5·8	1·5[h]
Scour indicators						
Active depth (m)				0·064	0·24	0·16
Number of indicators				32	45	22
Active width (m)[i]				7·0	11·8	4·5
Tracers						
Active depth (m)[e,h,j]				0·14	0·16	0·14
Number of mobile tracers[g]				18	48	40
Active width (m)[e,g]				4·5[k]	6·7	5·6
Subreach 2[d]						
Stream power ($W m^{-1}$)				2030	4160	2050
Mean travel distance (m)				49·3[l]	43·7[f]	70·3[m]
Number of mobile tracers[g]				154	53	26
Virtual velocity ($m h^{-1}$)				1·7[h]	2·0	2·1[h]
Scour indicators						
Active depth (m)				0·074	0·17	0·077
Number of indicators				18	35	26
Active width (m)[i]				3·9[n]	7·9	6·2
Tracers						
Active depth (m)[h,j]				0·062[k]	0·089	0·077
Number of mobile tracers[g]				152	77	65
Active width (m)[g]				4·5[k]	4·4	4·3
Subreach 3[d]						
Stream power ($W m^{-1}$)	1340	1660	1190	964	1980	975
Mean travel distance (m)	129·1[l]	98·5[f]	58·4[m]	26·8[m]	69·1[f]	25·8[m]
Number of mobile tracers[g]	50	152	149	43	49	11
Virtual velocity ($m h^{-1}$)	2·0[e]	3·8	1·1[e]	1·8	3·2	0·78[e]
Scour indicators						
Active depth (m)		0·078	0·063	0·053	0·084	0·047
Number of indicators		50	42	37	53	35
Active width (m)[i]		5·0[n]	4·9	4·9	6·2	4·2
Tracers						
Active depth (m)[h,j]	0·057[k]	0·074	0·075	0·044	0·11	0·082
Number of mobile tracers[g]	51	200	285	98	90	37
Active width (m)[g]	4·8[k]	5·1	5·1	4·4	5·6	4·3

[a] Dates of peak flow: A, 29/08/91; B, 19/11/91; C, 29/01/92; D, 20/10/92; E, 24/01/93; F, 04/03/93
[b] Flooding periods with more than one significant flood event indicated by italics; associated virtual velocities adjusted; see text for explanation
[c] Based on study reach
[d] The number of tracers used to define travel distances and active depth within a given subreach differ primarily because active depths are based on averages of scour and fill activity, which increases the number of tracers used
[e] Includes tracers deployed prior to this study; see Hassan and Church (1994)
[f] Tracers incoming and within subreach
[g] Includes only those tracers that moved a minimum distance of 1 m
[h] Adjusted value shown; see text for explanation
[i] See Figure 1 for number of cross-sections
[j] Includes depth observations equal to zero for immobile surface tracers within the defined active width
[k] Based only on tracers associated with fill activity
[l] Tracers incoming to subreach
[m] Tracers within and outgoing from subreach
[n] Mean excludes one cross-section that showed no scour activity

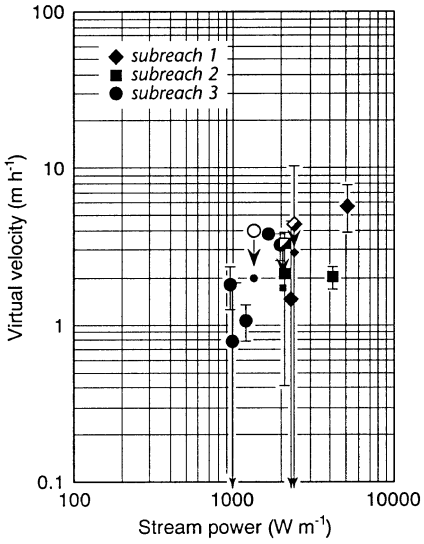

Figure 2. The relation between virtual velocity and maximum stream power. Open symbol indicates data derived from tracers that began from unconstrained surface positions during the first flood after tracer deployment. Such tracers can achieve longer travel distances than ones beginning from natural positions in the bed. This velocity was adjusted downward by 0·5 by using the mean of the ratios of mean travel distances of naturally constrained to unconstrained tracers observed in previous studies (data in Hassan and Church, 1992, table 8.4). Partially open symbol indicates data derived from newly placed tracers and ones starting from natural streambed positions. Velocities associated with newly deployed tracers were adjusted downward by 0·5; this involved 25 and 96 per cent of the observations for subreaches 1 and 2, respectively. Large solid symbol indicates all tracers began from natural streambed positions; small solid symbol indicates an adjusted result. Error bars indicate a two standard error range about the mean

the relatively low velocity of 2·0 m h^{-1} at about 4000 W m^{-1} reflects the influence of a constraint on the maximum distance that can be recorded by individual tracers. For this particular velocity, which is based on tracers entering and rearranged within subreach 2, the maximum distance between the nearest deployment area and the downstream boundary of the subreach is only 100 m. Although tracers deployed from the upstream area will eventually enter the subreach in greater number, the majority of tracers originated from the lower deployment area during this study (Figure 1; Table I). Hence, individual observations of travel distances could not exceed 100 m during this flooding period, which resulted in an underestimated mean travel distance and associated virtual velocity. Travel distances associated with large flood peaks, such as flooding period E of this example, would be proportionally more affected by this constraint because a larger portion of tracers would be expected to exceed the maximum distance that can be observed. Travel distances and associated virtual velocities based on the tracers rearranged within and leaving a subreach can also be constrained but, in this situation, the distance searched downstream of a given subreach limits the travel distances that can be observed. Overall, mean travel distances in this study are best described as lower bound estimates.

Some of the scatter evident in velocities may result from utilizing different subpopulations of tracers for the various flooding periods. For example, tracers transported into a subreach from upstream could represent more deeply buried particles and, hence, travel distances might be relatively reduced compared to distances from tracers exiting the subreach from relatively shallow burial depths. In the only direct comparison that is possible of marked stones travelling into and within with those moving within and out of a subreach, the mean travel distances differ by 3·8 m, which translates into a velocity difference of about 0·3 m h^{-1} for the given flooding period. This difference is an order of magnitude smaller than the standard deviation in the travel rate associated with this flooding period, as well as those associated with the majority of the virtual velocities. Nonetheless, any bias incorporated into the other mean travel distances cannot be quantified and remains a possible factor contributing to the variability exhibited around the general trend.

Tracer size distributions used to determine virtual velocity are not strictly identical between subreaches and between flooding periods, which may introduce bias into estimates. In flooding period E, the extreme case, the

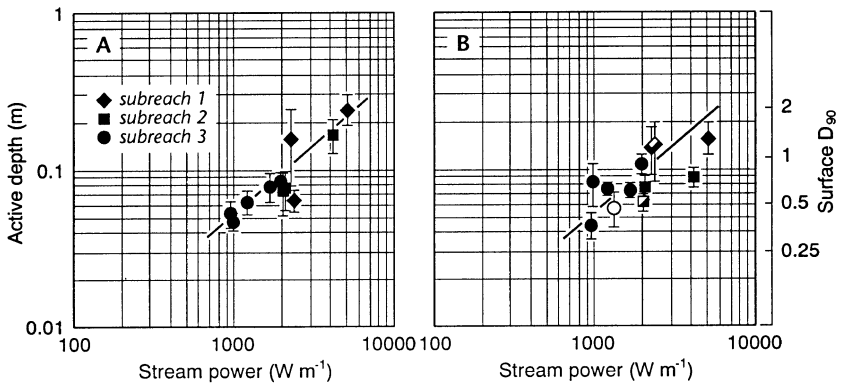

Figure 3. The relation between active depth and maximum stream power: (A) from scour indicators and (B) from tracer observations. Symbols as in Figure 2. The trend line, fitted by eye in (A), is repeated in (B) to permit comparison of the data sets. Error bars indicate a two standard error range about the mean; no error bar indicates that the error falls within the space occupied by the symbol

median diameter in subreach 2 is about two times larger than those in subreaches 1 and 3. The proximity of subreach 2 to the lower deployment area (Table I) facilitated the relatively rapid appearance of a larger proportion of large tracers compared to the other two subreaches. Although the remaining distributions exhibit some differences in the proportion of the two largest size fractions, particularly those associated with the first flood after tracer deployment, median diameters are, in general, comparable.

As a rule, relatively large particles exhibit larger recovery rates than smaller sizes because larger sizes tend to remain near or at the bed surface and are more readily found. If fractional recovery rates dictate that the population of tracers constituting the basis for virtual velocities is biased toward the larger tracers, which travel shorter mean distances, then virtual velocities may be underestimated. On the other hand, fractional recovery rates tend to reflect the arrival of various sizes within the subreaches as a function of distance from deployment areas. Smaller tracers tend to move longer distances, on average, than larger ones (Church and Hassan, 1991), so they turned up in the study subreaches soon after deployment. In comparison, recovery rates decreased for tracers 64 mm and larger for the first four flooding periods. The absence of one or both of the two largest sizes in some of the tracer distributions suggests that the associated virtual velocities may be slightly elevated. However, the 128 and 180 mm fractions comprise only 5 and 2 per cent of the gravels, respectively, and, therefore the net effect on virtual velocities should be minimal. In the latter two flooding periods, recovery rates tended to stabilize to an essentially constant rate for all size fractions because there had now been a sufficient number of competent flows to move coarse tracers from the deployment areas into the subreaches. Overall, the tracer size distribution found within a given subreach will evolve over time as a consequence of the finite populations deployed from restricted starting zones.

Bed morphology can exert an influence over tracer pathways (Sear, 1996). In this study, tracers were found distributed in pool, riffle and bar areas of the bed. About 80 per cent of tracers recovered were deposited in pools and adjacent gravel bars, which constitute the majority of the bed area spatially. This pattern is exhibited with a small number of tracers within a given subreach but is more convincingly displayed when observations reach a minimum of around 40. Once scoured, tracers tend to travel to pool areas regardless of the morphology of their starting positions. Using four datasets that consist of more than 50 observations and characterize the relatively low peak discharges of flooding periods C, D and F, 72 per cent of all tracers moved between pool areas. Only 32 per cent of the tracers that were mobilized from riffles were redeposited in this subunit of the bed morphology. When individual size fractions are examined, the majority of each size (>60 per cent) moved from pool to pool.

There is not a strict differentiation of tracer mobility based on bed morphology. Within the four 50+ observation data sets, tracers beginning in pools displayed greater mobility in two cases, while tracers originating in riffles exhibited greater mobility in the remaining cases. Overall, virtual velocities incorporate any bias introduced by bed morpholpogy because tracers originate from all areas of the bed, but no gross bias was detected.

Hassan *et al*. (1992) constructed a power function relating virtual velocity to excess stream power using data from numerous rivers. These virtual velocities, based primarily on unconstrained surface tracers, range from about 0·5 to as much as 100 m h^{-1}. In Carnation Creek, sediment travels between 0·78 and 5·8 m h^{-1} for the range of flows observed (Table II). Although 25 per cent of the velocities determined involve tracers beginning from unconstrained surface positions, adjustment of these observations compensates for the larger travel distances experienced by unconstrained tracers. The vertical exchange of material during floods should influence v_b and d_s reciprocally when determining rates of sediment transport (Hassan *et al*., 1992), which implies that the rate of increase in virtual velocity with stream power should lessen at higher values of stream power with respect to the rate of increase in active depth. When one prominent velocity outlier is ignored, data in Figure 2 imply, to some degree, that the rate of increase of virtual velocity with stream power lessens at the highest stream power recorded. However, this appearance is created by a single observation that is based on a relatively small sample of tracers. More data are needed before the reciprocal relation between virtual velocity and active depth can be quantified rigorously.

Depth of the active layer

Mean active depth based on scour indicators increases with stream power (Figure 3A; Table II). A relatively large difference in depth exists for two flooding periods with a similar stream power of about 2300 W m^{-1} in subreach 1. The elevated active depth of 0·16 m reflects continued adjustment of the talweg following the largest flood peak observed during the field programme. Concentrated scour in the low-flow channel in this subreach completed a lateral shift in position within stable channel banks. Overall, variation in active depth values has been reduced by averaging scour and fill depths for each flooding period (cf. Laronne *et al*., 1992). Two cases incorporate observations at inactive scour indicators. During flooding period B in subreach 3 and flooding period D in subreach 2 one cross-section registered no scour activity. To account for these observations, reach-averaged estimates of average depth were in each case adjusted by adding two zeros to depth observations. This reflects the likely number of inactive scour monitors within the expected active width (less than 6 m), given scour indicator spacing.

Mean active depth derived from tracers also increases with stream power (Figure 3B; Table II). For each flooding period, scour and fill depths were averaged to determine the active depth except when tracers were not already present in the subreach and only fill depths were available (Table II). When only scour depth defines active depth, the sequence of flood peak magnitudes introduces some bias into estimates by controlling the distribution of tracer burial depths available for a subsequent flood. When a relatively small peak precedes a larger peak in the flood sequence, the smaller flood buries tracers at relatively shallow depths compared to a larger flood and defines the upper limit of scour depths that can be observed in the subsequent, larger flood when more deeply buried tracers are not present in the channel reach. The effect of flood sequence is particularly pronounced in subreach 3, flooding periods A and B, and subreach 2, flooding periods D and E. Hence, fill depths reflect the magnitude of the flood peak more effectively and averaging scour and fill depths helps reduce the bias introduced by the sequence of flood magnitudes.

When the two techniques are compared, the relation based on tracers is less sensitive and exhibits greater variability than the relation based on scour indicators. Mean depths for relatively low stream powers are roughly similar (Figure 3). In subreach 1, the large difference in active depths for flooding period D (Table II) reflects the influence of tracers that have been vertically mixed within sediment over three flood seasons, which increased the observation of active depth derived from tracers. At larger stream powers, scour indicators record larger active depths than tracers, which is expected given that scour indicators record the maximum scour depth and associated net fill, while tracers record depths that are equal to or less than the maximum scour depth and net fill at the time of tracer emplacement. Nonetheless, the Wilcoxon signed rank statistic indicates that, over the range of the measurements, the two techniques do not produce significantly different estimates of mean active depth ($p = 0{\cdot}80$). In only one case did scour approach the nominal detection limit of 1 m in these three subreaches, so bias from this source is unlikely to be significant.

At the lower observed stream powers, the streambed is activated, in general, to a minimum depth of $0{\cdot}40D_{90}$ of surface sediment. At the largest peak discharge observed, a range of bed activity is exhibited in the three subreaches. Mean active depth equals 2·0, 1·4 and $0{\cdot}7D_{90}$ in subreaches 1, 2 and 3, respectively. These

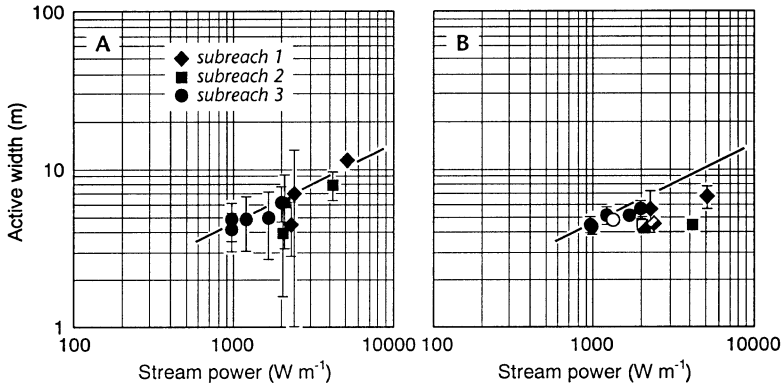

Figure 4. The relation between active width and maximum stream power: (A) from scour indicators and (B) from tracers. Symbols as in Figure 2. The trend line to permit comparison of results is based on (A). Error bars indicate a two standard error range about the mean

differences probably reflect relative stream power amongst subreaches for a given peak discharge which is controlled, in part, by local channel gradient (Table I). The result in subreach 1 suggests that active depth may exhibit an upper limit near $2D_{90}$ (Wilcock and McArdell, 1997). The possibility exists for deep burial (>1m) at the avalanching face of a gravel bar. But the bars remained essentially stationary except during the largest flood observed, when some bars advanced, on average, by several metres. Once tracers have been subjected to a sufficient number of large-magnitude floods, they should be found deeply buried within channel sediment because of thorough vertical mixing (Hassan and Church, 1994) and flood-sequence bias should lessen. By the end of the field programme, the necessary vertical mixing appears to have been achieved in all subreaches for the range of flow magnitudes observed.

Width of the active layer

Mean active width based on scour indicators increases with stream power (Figure 4A; Table II). One observation of width in subreach 2 deviates prominently below the general trend at about 2000 W m^{-1}. It is not clear why the individual cross-section widths were relatively small compared to those of the other flooding periods. The corresponding active width based on tracer movement does not appear to be anomalous (Figure 4B; Table II). The maximum channel width did not become fully engaged even during the highest discharge peak but, rather, the majority of sediment movement was concentrated in 67, 74 and 64 per cent of the streambed width in subreaches 1, 2 and 3, respectively. Smaller flows activated about 44 per cent of the potential streambed width (Table I).

Mean active width derived from tracers displays little sensitivity to stream power (Figure 4B; Table II) in contrast to active width based on scour indicators. Scour and fill widths for a given flooding period were averaged because an overall improvement in the pattern of active width was achieved. Adjustment of the apparent active width between the smallest and largest flood peak equalled 2 and 1m in subreaches 1 and 3, respectively. In subreach 2, tracers appeared to move through a comparatively small width (Table II) which essentially did not change with flood magnitude.

Active widths based on scour indicators are roughly comparable to those derived from tracers for relatively small active widths (<6m) (Figure 4). When the width of channel activity increases, widths recorded by scour indicators exceed those determined by tracers. Nonetheless, the Wilcoxon signed rank statistic indicates that, over the range of measurements, the two techniques do not yield significantly different active widths ($p = 0{\cdot}18$).

Porosity

No direct measurements were carried out in Carnation Creek – indeed, few measurements of porosity have ever been made of naturally deposited stream gravels in the field. Bed material porosity was estimated at 0·2 using the porosity–particle size relation developed by Carling and Reader (1982) for poorly sorted, consolidated channel sediment. The general nature of bed sediment in Carnation Creek indicates that this relation is more

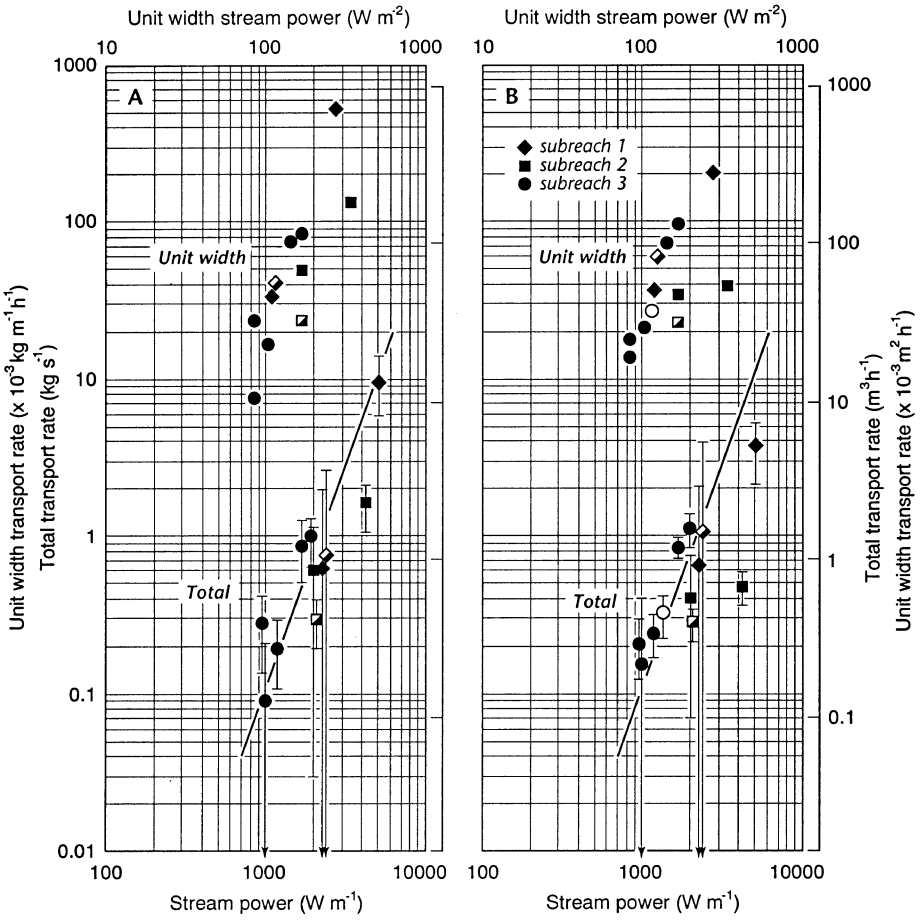

Figure 5. The relation between transport rate and stream power: (A) using scour indicators and (B) using only tracers. Symbols as in Figure 2. Trend line, arbitrarily drawn with exponent 2·5, permits comparison of results. Error bars (kg s^{-1}) indicate a two standard error range about the observations

appropriate than the other available relation formulated by Komura (1961), which characterizes well-sorted, recently deposited sediment. Porosity remains, in general, a poorly characterized variable in sediment flux calculations. Since it is a constant in our calculations, the assigned value may be a source of bias, but not of variability.

TRANSPORT RATES

Total sediment flux

Bed material transport rates generally reflect the magnitude of stream power (Figure 5). Rates range from 0·090 to 9·7 kg s^{-1} when the active layer is defined by scour indicators (Table III) and establish a relatively sensitive trend with stream power (Figure 5A). Transport rates of 0·29 and 1·61 kg s^{-1} in subreach 2 are underestimated because of the negatively biased active width and virtual velocity, respectively, previously discussed. Transport rates based on tracers alone exhibit a narrower range, 0·16 to 3·7 kg s^{-1} (Table III). As might be expected from the discussions of active depth and width, these transport rates show a less sensitive trend with stream power (Figure 5B).

Transport rates expressed in volumetric terms more effectively connect the movement of bed material to channel morphology. Accordingly, volumetric scales are included in both Figure 5 and Table III. For the

Table III. Bed material transport rates, Carnation Creek

Flooding period*	A	B	C	D	E	F
Subreach 1						
Stream power ($W m^{-1}$)				2360	5090	2250
Unit width stream power ($W m^{-2}$)				129	278	123
Scour indicators						
Total transport rate ($kg s^{-1}$)				0·76±0·97	9·72±1·96	0·62±0·67
Total transport rate ($m^3 h^{-1}$)				1·03±1·32	13·2±2·67	0·84±0·93
Unit width transport rate ($kg m^{-1} s^{-1}$)				0·042	0·53	0·034
Unit width transport rate ($m^2 h^{-1}$)				0·056	0·72	0·046
Tracers						
Total transport rate ($kg s^{-1}$)				1·10±1·37	3·74±0·79	0·66±0·70
Total transport rate ($m^3 h^{-1}$)				1·49±1·86	5·08±1·08	0·89±0·96
Unit width transport rate ($kg m^{-1} s^{-1}$)				0·060	0·20	0·036
Unit width transport rate ($m^2 h^{-1}$)				0·082	0·28	0·049
Subreach 2						
Stream power ($W m^{-1}$)				2030	4160	2050
Unit width stream power ($W m^{-2}$)				166	341	168
Scour indicators						
Total transport rate ($kg s^{-1}$)				0·29±0·050	1·61±0·27	0·60±0·29
Total transport rate ($m^3 h^{-1}$)				0·39±0·068	2·18±0·36	0·82±0·39
Unit width transport rate ($kg m^{-1} s^{-1}$)				0·024	0·13	0·050
Unit width transport rate ($m^2 h^{-1}$)				0·032	0·18	0·067
Tracers						
Total transport rate ($kg s^{-1}$)				0·28±0·031	0·47±0·053	0·41±0·17
Total transport rate ($m^3 h^{-1}$)				0·38±0·041	0·63±0·072	0·56±0·23
Unit width transport rate ($kg m^{-1} s^{-1}$)				0·023	0·038	0·034
Unit width transport rate ($m^2 h^{-1}$)				0·031	0·052	0·046
Subreach 3						
Stream power ($W m^{-1}$)	1340	1660	1190	964	1980	975
Unit width stream power ($W m^{-2}$)	114	142	102	82	169	83
Scour indicators						
Total transport rate ($kg s^{-1}$)		0·88±0·19	0·20±0·044	0·28±0·069	0·99±0·18	0·090±0·063
Total transport rate ($m^3 h^{-1}$)		1·19±0·26	0·27±0·060	0·38±0·093	1·34±0·24	0·12±0·086
Unit width transport rate ($kg m^{-1} s^{-1}$)		0·075	0·017	0·024	0·084	0·0077
Unit width transport rate ($m^2 h^{-1}$)		0·011	0·023	0·032	0·11	0·010
Tracers						
Total transport rate ($kg s^{-1}$)	0·32±0·047	0·84±0·059	0·24±0·037	0·21±0·041	1·14±0·15	0·16±0·12
Total transport rate ($m^3 h^{-1}$)	0·44±0·064	1·15±0·080	0·33±0·050	0·29±0·055	1·54±0·21	0·22±0·16
Unit width transport rate ($kg m^{-1} s^{-1}$)	0·027	0·072	0·021	0·018	0·097	0·014
Unit width transport rate ($m^2 h^{-1}$)	0·037	0·098	0·028	0·024	0·13	0·019

* Notation as in Table II

flooding periods containing the smallest and largest peak discharge observed, the total volume of sediment moved in the subreaches equalled 27 and 360 m^3, respectively, when the active layer is defined by scour indicators.

The two methods yield comparable rates of transport except in three instances. During flooding period E, rates derived from scour indicators exceed those determined from tracers by 6·0 and 1·1 kg s^{-1} in subreaches 1 and 2, respectively. Differences in both active depth and active width contributed to this outcome. In contrast, tracers produced a larger rate by 0·34 kg s^{-1} during flooding period D in subreach 1 because of the order of magnitude difference in active depth between the two techniques (Table II). When these cases are not considered, transport rates differ by an average of 0·10 kg s^{-1}. The Wilcoxon signed rank statistic indicates that, over the range of measurements, transport rates based on the two measurement techniques do not differ statistically ($p = 0·72$).

Error analysis

Errors in estimates of virtual velocity, active depth and active width lead to uncertainty in transport rates. It is assumed that the errors associated with the selected porosity and sediment density are negligible in comparison with other errors. Error analysis followed general rules for the propagation of error when deriving a quantity from multiple measured quantities (Beers, 1957). The uncertainty in transport rate is calculated by:

$$E_{\mathrm{n}} = \sqrt{\sum_{i=1}^{n} \left\{ \left(\frac{\partial G_{b_i}}{\partial v_b} \delta v_b \right)^2 + \left(\frac{\partial G_{b_i}}{\partial d_s} \delta d_s \right)^2 + \left(\frac{\partial G_{b_i}}{\partial w_s} \delta w_s \right)^2 \right\}} \tag{3}$$

where δv_{b} is the uncertainty of the virtual velocity estimate, δd_{s} the uncertainty of the active depth estimate, and δw_{s} the uncertainty of the active width estimate for $i = 1$ to n observations. Uncertainty in the three variables can be estimated from standard errors. Partial derivatives of G_{b} and $\mathrm{v_b}$, $\mathrm{d_s}$ and $\mathrm{w_s}$, respectively, are determined from Equation 1. Results depend straightforwardly on measurement errors because all terms are linear.

Transport rates for subreach 1 exhibit the largest errors (Figure 5; Table III) in both sets of estimates. In two of the three estimates, the error exceeds the transport rate. Over all the tracer-based rates, uncertainty in velocity estimates accounts for an average of 65 per cent of the transport rate error. Active depth and width contribute, on average, 24 per cent and 11 per cent, respectively. Uncertainty in rates based on scour indicators also derives, in large part, from velocity estimates, which introduce, on average, 51 per cent of the error. Active depth and width estimates contribute approximately equally to the uncertainty. In general, relatively large standard errors result from the relatively small samples (Table II), given the variability present in the measurements.

The error estimates given here incorporate random variation which arises from the stochastic nature of bed material transport and a portion of 'local bias' – bias which is associated with an individual observation (as, for example, when virtual velocities may be underestimated because of limited tracer recovery). However, the mean of local biases, if it happens to be non-zero, is not captured. Nor do the calculations include general bias, such as might be associated with the porosity specification.

Unit width sediment flux

Total fluxes were converted to unit width fluxes (Table III) using mean bankfull width of each subreach (Table I). Overall, trends between unit width flux and stream power in the three subreaches collapse onto one general trend (Figure 5), as we would expect for similar materials subject to similar mobilizing forces. The two notable outliers in subreach 2, previously identified in relation to total transport rates, are still evident in both the scour indicator and tracer-based trends. When fluxes based on scour indicators are considered, rates range from a minimum of $0{\cdot}0077\,\mathrm{kg\,m^{-1}\,s^{-1}}$ at $83\,\mathrm{W\,m^{-2}}$ in subreach 3 (flooding period F) to a maximum of $0{\cdot}53\,\mathrm{kg\,m^{-1}\,s^{-1}}$ at $278\,\mathrm{W\,m^{-2}}$ in subreach 1 (flooding period E). Fluxes based on tracers give a more restricted range, as expected from total flux calculations (Table III).

If the aim is to determine an average transport rate over the competent portion of the streambed, active width rather than total channel width should be used to determine transport rate per unit width. In this study, rates increase, on average, by 1·53 times (subreach 2, flooding period D outlier excluded) when the scour indicator active width is used in computations. The typical standardization of rates using wetted channel width stems from the impracticality in most studies of defining the actual active width.

DISCUSSION AND CONCLUSIONS

Transport rates derived using virtual velocity characterize the gravel portion of channel (subsurface) bed material. In Carnation Creek, the calculated transport rates apply strictly to 63 per cent of channel sediment because travel distances of particles smaller than 16 mm were not directly monitored (27 per cent of gravels). However, Church and Hassan (1992) have shown that the sensitivity of travel distance to particle size lessens as size decreases below the median diameter of subsurface sediment. Haschenburger (1996) confirmed the

validity of their heuristic travel distance–particle size relation in Carnation Creek using three different populations of tracers, and Wilcock (1997) has offered a physical explanation for the relation.

A direct evaluation of the effect on estimated virtual velocities in Carnation Creek of ignoring smaller gravels can be accomplished for flooding period D by estimating mean travel distances for the finer range of gravels not directly monitored – the 2 to 11 mm fractions – and incorporating these into an estimate of overall mean travel distance for gravels during the flooding period. The fractional mean travel distances were determined by formulating a travel distance–particle size relation for data representing the same flooding period considering only mobile tracers. This represents a departure from the Church–Hassan relation that considers all tracers but achieves more appropriate estimates of virtual velocity. The resulting travel distance–particle size relation exhibits a trend similar to that of the Church–Hassan relation.

The mean travel distance representing all gravels is 3·7 m larger than that estimated by tracer sizes only. The associated increase in virtual velocity is 0·25 m h^{-1}, which is an order of magnitude smaller than the typical standard deviation associated with virtual velocities for this flooding period (and all other flooding periods). Thus, it appears that mean travel distances based on the tracers adequately represent the displacement of gravels present in the channel bed material in Carnation Creek and the calculated transport rates then apply to 90 per cent of channel sediment. Accordingly, it appears reasonable to assert that the tracers represent the transport of the true bed material, the 10 per cent of smaller sizes likely representing trapped fines.

There remains a question of whether some bias would arise in any attempt to extend the calculations to estimate total bed material flux over a sequence of events. It is possible that material finer than 16 mm moves rather more frequently because it is displaced at low flows. Our experience, and that of other investigators, is that the threshold for effective gravel movement is rather sharp, and that, then, all sizes move. At moderate flows, however, transport does appear to be weighted toward smaller sizes (i.e. to be in the partial transport regime of Wilcock and McArdell, 1997).

The resulting transport–flow relations for Carnation Creek are encouraging in that they replicate, in general, what is known about sediment transport–flow relations in gravel-bed rivers derived from conventional sampling approaches. In particular, the substantial sensitivity of the transport to stream power is typical for gravel transport near the threshold for significant transport. Error analysis indicates that more precise transport estimates would be achieved by increasing the number of tracers used to estimate travel distance and the corresponding virtual velocity. However, it should be emphasized that variability in active depth and width variables was reduced in this study by averaging scour and fill estimates together, which actually increased the number of observations upon which most mean values were calculated. Increased sample sizes reduce uncertainty by lowering standard errors. In addition, bias introduced into virtual velocities through grain size-related effects, through bed morphology, and through the physical constraints of distance between tracer deployment areas and observation areas, and of the downstream boundary of recovery procedures can be minimized by careful consideration of field sampling design. Future field sampling strategies should be adjusted accordingly.

Recovering tracers within relatively short channel lengths (in this study, seven times the average bankful width) can lead to relatively small sample sizes, depending on the number of tracers deployed, the distance between deployment area and searched channel reach, and the time elapsed since deployment. It is possible to increase the sample size upon which virtual velocities are based by pooling all tracer trajectory data from the three subreaches for a given flooding period to derive an overall, reach-wide estimate for the latter three flooding periods. Resulting virtual velocities equal 1·8, 4·2 and 1·7 m h^{-1} in flooding periods D, E and F, respectively. Given that the virtual velocity associated with flooding period E in subreach 2 departs significantly from the general trend, these data were excluded from the pooled estimate. Standard errors are lowered by an order of magnitude in flooding periods D and F, while the standard error for flooding period E is about the same as the mean of the standard errors associated with individual subreach estimates.

Corresponding reach-based transport rates are not statistically different from those rates calculated using individual subreach estimates of virtual velocity, whether based on scour indicators ($p = 0{\cdot}80$) or tracers ($p = 0{\cdot}77$; Wilcoxon signed rank statistic).

One further observation is worth mention in regard to reach-wide virtual velocities. After flooding period D, tracer recovery was carried out for the complete study reach downstream of the upper deployment area (*c*.

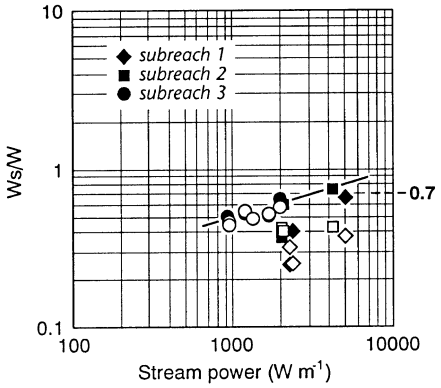

Figure 6. The relation between relative active width, w_s/w, and maximum stream power. The trend line defines a relatively insensitive upper envelope for estimates of active width. Solid symbols: scour indicators; open symbols: tracers.

750 m), making it possible to derive an estimate of virtual velocity over this longer channel reach. Using only tracers that were vertically mixed within the streambed for one flood season prior to this flooding period, the virtual velocity equals 1·6 m h^{-1}, which is only slightly lower than individual subreaches and the pooled estimate. This estimate is based on 280 mobile tracers, although the recovery yielded a sample of 704 tracers.

Virtual velocities were recomputed using a threshold discharge of 8 m^3 s^{-1} to explore the effect on estimates of a shorter period of presumed particle movement. At this discharge, transport rates near the WSC streamflow gauging station (0·22 kg s^{-1}, 0·31 m^3 h^{-1}) are an order of magnitude larger than the rate determined for 4 m^3 s^{-1}, although channel bed scour still extends to a mean depth of less than 1 cm in the study reach. The 8 m^3 s^{-1} baseline discharge decreases the duration of competent flow by about 9 h, on average (that is, by near 40 per cent), and results in a mean increase in virtual velocities of 1·4 m h^{-1}. When increases in velocity are compared individually with the associated standard deviations of the 4 m^3 s^{-1} baseline, 83 per cent of these increases are smaller. The remaining two increases, which are associated with the largest changes in the flow duration between threshold discharge magnitudes, are within the same order of magnitude as the standard deviations.

Field measurement strategies could be employed to document gravel movement during flood events to more precisely define the period of particle motion. This would require the use of bedload samplers or acoustic devices (e.g. Hollingshead, 1971; see also Thorne, 1986) and the presence of personnel during flood events, which nullifies one of the advantages of the virtual velocity approach. In the case of gravel-bedded Turkey Brook (Reid and Frostick, 1984), where the onset of sediment motion occurred at a flow higher than termination so that a reduction in the active time was introduced relative to that for a common threshold, the effect on the total period of sediment motion is minimal. It was shortened by only one hour, on average, which amounts to a 10 per cent reduction of the period of competent flow. At this stage, it appears that the magnitude of potential error which may be introduced as a consequence of not directly documenting the period of particle motion does not justify a large field effort to repair, so long as entraining flows are approximately known.

Transport rates determined using data from scour indicators display a more consistent trend with stream power than those determined from tracers alone. Nonetheless, if the primary study objective is simply to estimate transport rates, it would appear to be more expedient to acquire all needed field data by using tracers. Tracers must be deployed to quantify the virtual velocity of bed material regardless of how the active layer dimensions are determined. Field time could be saved by not installing and recovering scour indicators after flood events. However, over the range of measurements in this study, active width defined by tracers was relatively insensitive to stream power, and relative active width as defined by the tracers is not consistently related to stream power at all (Figure 6). Therefore, a further practical compromise might be to simply assume for all stream powers an active width of 0·7 times the total channel width (the average maximum active width for the three subreaches in this study; see Figure 6). The envelope of values in Figure 6 varies by about ±12 per cent about this value. In Carnation Creek, calculations assuming a constant active width yield slightly higher transport rates for small stream powers, as might be expected when the difference between the assumed and measured active width is the largest. Nonetheless, the Wilcoxon signed rank statistic indicates that, over the

range of measurements, these transport rates do not differ significantly from those with active layer dimensions defined by scour indicators ($p = 0{\cdot}25$). The applicability of this expedient field strategy requires confirmation in other gravel-bed rivers, where attention could usefully be given, as well, to determining the number of tracer particles required to achieve various levels of precision.

Given the technology currently available to trace particles and determine active layer dimensions, the virtual velocity approach can be applied in gravel-bed rivers only where the channel bed is accessible for recovery procedures. The streambed must be dry or flow significantly reduced for periods sufficiently long to allow recovery of tracers and scour indicators. Nonetheless, the approach appears to be more flexible in smaller channels than conventional sampling approaches because bridges or boats are not required and personnel need not be present during flood events.

Tracing individual particles to determine their virtual velocity also provides information about fundamental transport processes, such as the vertical exchange of various sediment sizes (Hubbell and Sayre, 1964). Conventional sampling at multiple cross-sections within a given river reach can yield information about mobile particle size distributions and differences in sediment flux between cross-sections, but little insight is gained about particle exchange, an important component in understanding the evolution of heterogeneous and variable streambeds. Further, traps and bridges used for portable sampler deployment are fixed in position, whereas the virtual velocity approach can be employed to gain an average (in some sense) over a desired channel reach. A two-way Friedman analysis of variance (Bradley, 1968) indicates that transport rates in Carnation Creek vary between subreaches ($p = 0{\cdot}097$) but not between techniques ($p = 0{\cdot}59$) when the three latter flooding periods are considered. These transport rates characterize reaches positioned within an overall study reach of only 900 m. Downstream variability (locally) has not been considered in most estimates of transport, even though it is the basis for the variation of fluvial morphology.

In this study, the two measurement techniques used to determine the dimensions of the active layer of the streambed returned comparable active depth, width and transport rates for the range of flow magnitudes observed. However, values tend to diverge more at higher stream powers, whilst the majority of observations are clustered in the lower range of stream power. Additional results for higher stream powers might modify the statistics. The estimation of volumetric bed material transport based on virtual velocity, active layer dimensions and sediment porosity has only recently been attempted in gravel-bed rivers. There remains substantial scope to refine the measurements. Given the results of this study, pursuit of the approach appears warranted.

ACKNOWLEDGEMENTS

Funding was provided by the Natural Sciences and Engineering Research Council of Canada (M.C.), the Geological Society of America (J.K.H.), and the J. Hoover Mackin Research Award, Quaternary Geology and Geomorphology Division, Geological Society of America (J.K.H.). The British Columbia Ministry of Forests provided logistical support by operating the Carnation Creek field station. Scott Babakaiff, Anthony Collett, Brett Eaton, Darren Ham, Blythe Killam, Craig Nistor, Marian Oden, Shannon Sterling, Kristie Trainor and Sid Tsang assisted with fieldwork. Some of the analysis was conducted whilst J.K.H. was a US National Research Council Postdoctoral Research Associate at the US Geological Survey, Boulder, Colorado. We thank the journal's anonymous reviewers for constructive comments which improved the manuscript.

REFERENCES

Bagnold, R. A. 1966. *An approach to the sediment transport problem from general physics*, US Geological Survey Professional Paper, **422-I**, 37 pp.

Bagnold, R. A. 1986. 'Transport of solids by natural water flow: evidence for a world-wide correlation', *Proceedings of the Royal Society of London, Series A*, **405**, 369–374.

Beers, Y. 1957. *Introduction to the Theory of Error*, Addison-Wesley, Reading, MA, 66 pp.

Bradley, J. V. 1968. *Distribution-free Statistical Tests*, Prentice-Hall, Englewood Cliffs, 388 pp.

Carling, P. A. 1987. 'Bed stability in gravel streams, with reference to stream regulation and ecology', in Richards, K. S. (Ed.), *River Channels: Environment and Process*, Institute of British Geographers Special Publications Series, Oxford, 321–347.

Carling, P. A. and Reader, N. A. 1982. 'Structure, composition and bulk properties of upland stream gravels', *Earth Surface Processes and Landforms*, **7**, 349–365.

Church, M. and Hassan, M. A. 1992. 'Size and distance of travel of unconstrained clasts on a streambed', *Water Resources Research*, **28**, 299–303.
du Boys, M. P. 1879. 'Etudes du regime et l'action exercé par les eaux sur un lit a fond de gravier indéfiniment affouiable', *Annales des Ponts et Chaussées*, **5**, 141–195.
Einstein, H. A. 1937. 'Bedload transport as a probability problem', in Shen, W. H. (Ed.), *Sedimentation*, Colorado State University, Ft Collins, C1–C105.
Engel, P. and Lau, L. 1981. 'The efficiency of basket type bed load samplers', in *Erosion and Sediment Transport Measurement*, IAHS Publication **133**, 27–34.
Ergenzinger, P. 1988. 'The nature of coarse material bed load transport', in *Sediment Budgets*, IAHS Publication **174**, 207–216.
Gomez, B. 1991. 'Bedload transport', *Earth-Science Reviews*, **31**, 89–132.
Graf, W. H. 1971. *Hydraulics of Sediment Transport*, McGraw-Hill, New York, 509 pp.
Haschenburger, J. K. 1996. *Scour and fill in a gravel-bed channel: observations and stochastic models*, PhD thesis, University of British Columbia, 144 pp.
Hassan, M. A. 1990. 'Scour, fill, and burial depth of coarse material in gravel bed streams', *Earth Surface Processes and Landforms*, **15**, 341–356.
Hassan, M. A. and Church, M. 1992. 'The movement of individual grains on the streambed', in Billi, P., Hey, C. R., Thorne, C. R. and Tacconi, P. (Eds), *Dynamics of Gravel-bed Rivers*, John Wiley & Sons, Chichester, 159–172.
Hassan, M. A. and Church, M. 1994. 'Vertical mixing of coarse particles in gravel bed rivers: a kinematic model', *Water Resources Research*, **30**, 1173–1185.
Hassan, M. A., Church, M. and Ashworth, P. J. 1992. 'Virtual rate and mean distance of travel of individual clasts in gravel-bed channels', *Earth Surface Processes and Landforms*, **17**, 617–627.
Helley, E. J. and Smith, W. 1971. *Development and Calibration of a Pressure-difference Bedload Sampler*, US Geological Survey Open-File Report, 18 pp.
Hoey, T. 1992. 'Temporal variations in bedload transport rates and sediment storage in gravel-bed rivers', *Progress in Physical Geography*, **16**, 319–338.
Hollingshead, A. B. 1971. 'Sediment transport measurements in gravel river', *Journal of the Hydraulics Division, American Society of Civil Engineers*, **97**, 1817–1834.
Hubbell, D. W. 1964. *Apparatus and Techniques for Measuring Bedload*, US Geological Survey Water-Supply Paper, **1748**, 74 pp.
Hubbell, D. W. and Sayre, W. W. 1964. 'Sand transport studies with radioactive tracers', *Journal of the Hydraulics Division, American Society of Civil Engineers*, **90**, 39–68.
Hubbell, D. W. and Stevens, H. H. 1986. 'Factors affecting the accuracy of bedload sampling', *Proceedings of the 4th Federal Inter-Agency Sedimentation Conference*, 4.20–4.29.
Komura, S. 1961. 'Bulk properties of river bed sediments, its applications to sediment hydraulics', *Proceedings of the 11th Japan National Congress for Applied Mechanics*, 227–231.
Kondolf, G. M. and Matthews, W. V. G. 1986. 'Transport of tracer gravels on a coastal California river', *Journal of Hydrology*, **85**, 265–280.
Laronne, J. B., Outhet, D., Duckham, J. L. and McCabe, T. J. 1992. 'Determining event bedload volumes for evaluation of potential degradation sites due to gravel extraction, N.S.W., Australia', in *Erosion and Sediment Transport Monitoring Programmes in River Basins*, IAHS Publication **210**, 87–94.
Laronne, J. B., Outhet, D. N., Carling, P. A. and McCabe, T. J. 1994. 'Scour chain employment in gravel bed rivers', *Catena*, **22**, 299–306.
Leopold, L. B. and Emmett, W. W. 1976. 'Bedload measurements, East Fork River, Wyoming', *Proceedings of the National Academy of Science*, **73**, 1000–1004.
Leopold, L. B., Emmett, W. W. and Myrick, R. M. 1966. *Channel and Hillslope Processes in a Semiarid Area, New Mexico*, US Geological Survey Professional Paper, **325G**, 61 pp.
Lisle, T. E. 1986. 'Stabilization of a gravel channel by large streamside obstructions and bedrock bends, Jacoby Creek, northwestern California', *Geological Society of America Bulletin*, **97**, 999–1011.
Madej, M. A. 1984. *Recent Changes in Channel-stored Sediment, Redwood Creek, California*, Redwood National Park Service Technical Report **11**, 54 pp.
Martin, Y. and Church, M. 1995. 'Bed-material transport estimated from channel surveys: Vedder River, British Columbia, *Earth Surface Processes and Landforms*, **20**, 347–361.
Milhous, R. T. and Klingeman, P. C. 1973. 'Sediment transport system in a gravel-bottomed stream', in *Hydraulic Engineering and the Environment*, American Society of Civil Engineers, 21st Annual Hydraulics Division Specialty Conference, 293–303.
Mosley, M. P. 1978. 'Bed material transport in the Tamaki River near Dannevirke, North Island, New Zealand', *New Zealand Journal of Science*, **21**, 619–626.
Parker, G. and Klingeman, P. C. 1982. 'On why gravel bed streams are paved', *Water Resources Research*, **18**, 1409–1423.
Reid, I. and Frostick, L. E. 1984. 'Particle interaction and its effect on the thresholds of initial and final bedload motion in coarse alluvial channels', in Koster, E. H. and Steel, R. J. (Eds), *Sedimentology of Gravels and Conglomerates*, Canadian Society of Petroleum Geologists, Memoir **10**, 61–68.
Reid, I., Layman, J. T. and Frostick, L. E. 1980. 'The continuous measurement of bedload discharge', *Journal of Hydraulic Research*, **18**, 243–249.
Schoklitsch, A. 1934. 'Der geschiebetrieb und die geschiebefracht [Bedload transport and bedload movement]', *Wasserkraft Wasserwirtschaft*, **4**, 1–7.
Sear, D. A. 1996. 'Sediment transport processes in pool–riffle sequences', *Earth Surface Processes and Landforms*, **21**, 241–262.
Shulits, S. 1935. 'The Schoklitsch bed-load formula', *Engineering*, June, 644–646, 687.
Slaymaker, H. O. 1972. 'Patterns of present sub-aerial erosion and landforms in mid-Wales', *Transactions of the Institute of British Geographers*, **55**, 47–68.

Tassone, B. L. 1987. 'Sediment loads from 1973 to 1984 08HB048 Carnation Creek at the mouth, British Columbia', in Chamberlin, T. W. (Ed.), *Proceedings of the Workshop: Applying 15 Years of Carnation Creek Results*, Pacific Biological Station, Nanaimo, British Columbia, 46–58.
Thorne, P. D. 1986. 'An intercomparison between visual and acoustic detection of seabed gravel movement', *Marine Geology*, **72**, 11–31.
Tripp, D. B. and Poulin, V. A. 1986. *The effects of logging and mass wasting on salmonid spawning habitat in streams on the Queen Charlotte Islands*, British Columbia Ministry of Forests and Lands, Land Management Report No. **50**, 29 pp.
Wilcock, P. R. 1993. 'Critical shear stress of natural sediments', *Journal of Hydraulic Engineering*, **119**, 491–505.
Wilcock, P. R. (1997). 'Entrainment, displacement, and transport of tracer gravels', *Earth Surface Processes and Landforms*, **22,** 1125–1138.
Wilcock, P. R. and McArdell, B. W. 1997. 'Partial transport of a sand-gravel mixture', *Water Resources Research*, **33**, 235–245.
Wilcock, P. R., Barta, A. F., Shea, C. C., Kondolf, G. M., Matthews, W. V. G. and Pitlick, J. 1996. 'Observations of flow and sediment entrainment on a large gravel-bed river', *Water Resources Research*, **32**, 2897–2909.

